Neural Correlate of Disembodied Cognition

Harshit Bockadia & Elizabeth B Torres

Abstract— Understanding brain connectivity patterns that may spontaneously emerge in response to biofeedback training remains of great interest to neuroscientists. Along those lines, Brain Computer Interfaces (BCI) mediated by EEG signals that dynamically evolve as the user attempts to control a cursor on the screen, has helped identify brain areas recruited during the learning process. There is an adaptive process that takes place between the computer algorithm and the solution that the brain arrives at to mentally control the instructed cursor direction through intentional thoughts. Using new personalized techniques, we here address how different participants learn during this co-adaptive process, in which bodily motions are curtailed in favor of mental motion. First, the person uses mental imagery of directional movements to attempt the cursor control, but as the computer algorithm and the brain work together to gain accuracy, this mental imagery reportedly reaches a different level of abstraction. Indeed, each participant reports that there is a point when they are mentally controlling the external computer cursor, yet no longer imagining the movement direction. We compared the evolution of a participant without proprioception owing to neuronopathy, to that of participants with intact afferent nerves. We found fundamentally different patterns of activation between the participants with intact bodily kinesthetic reafference and the participant without proprioception. In the latter, the connectivity patterns were far higher and distributed across the entire brain during the initial stages of learning, in contrast to the other participants. Furthermore, the changes across learning stages were more pronounced in the neuronopathy case. We infer from this result that in the absence of kinesthetic reafference, heavy reliance on other senses like vision and hearing, may endow the brain with higher capacity to handle the excess cognitive load. In the absence of proprioception, we may be able to quantify this capacity through the evolution of the stochastic patterns of EEG variability within BCI co-adaptive learning.

Index Terms—*Brain Computer Interface, EEG, weighted directed graphs, brain connectivity, earth mover's distance*.

I. INTRODUCTION and RELATED WORK

Every purposeful action self-generated by our nervous system is guided by mental intent and, when appropriate, feedback continuously flows from the peripheral (PNS) to the central nervous system (CNS). Under such conditions, mental intent to perform an action results in physical volition, controlling through that action, our surrounding environment at will [1-3]. In this sense, we have agency over our thoughts, decisions and voluntary actions because we can clearly establish a link between the cause of our impending actions and their possible sensory consequences. In intact nervous systems, this map between actions and sensory consequences seems to develop from infancy and be adapted and updated as we continue to learn largely beneath awareness, to master a predictive code that helps overcompensate for transduction and transmission sensory-motor delays throughout the nervous systems [4,5]. Here we explore some of the activation patterns that take place as participants successfully master the volitional control of an external cursor's direction at will.

II. MATERIALS AND METHODS

A. Participants

This study involved twenty-one college level participants (13 males and 8 females, ages: 29.00 ± 7.01). Among these, we had one special participant IW, a 61-year-old left-handed man who lost proprioception at 19 and has not recovered from this neuronopathy since then [6-9]. He cannot sense touch, pressure, body position or body motion and as such, does not have kinesthetic reafference. He lacks sensory and motor reflexes. All the participants in this study signed the consent form approved by the Rutgers University Institutional Review Board (IRB) in compliance with the Declaration of Helsinki.

B. Experimental Setup

Figure 1 shows the setup. Subjects wore a cap to measure electro-encephalographic (EEG) activity recording 64 channels at a sampling rate of 256 Hz. The BioSemi System uses an international 10-20 convention. Details on this high resolution biopotential measurement found at http://www.biosemi.com/index.htm. The EEG activity is recorded in response to imagining the instructed direction (left or right) as if intending to move the computer cursor towards left or right. Quite often, selective functionality is set a priori for brain regions of interest (RoI) and those regions are fine-tuned based on the task to be performed. Here, we let the (BCI) signal evolve in response to the Bayesian sparse probit classifier, which automatically fine-tunes the brain region that maximizes performance accuracy [10,11]. In this sense, the RoI ***self-emerges*** as the brain learns the cursor control task [12].

The task is divided into three phases: (1) training, open-loop (no feedback from the performance) where we estimate the currents but do not yet train the classifier algorithm; (2) training, closed-loop (real time feedback from the performance) where both the participant and the classifier algorithm are trained; (3) testing, based on real-time loops connecting our sensory inputs and motor outputs, whereby the efferent flow of information from the CNS to the PNS is constantly updated. Part of the update relies on kinesthetic reafference [4] and proprioception. In the absence of these re-entrant activity, we know that the brain learns to sensory substitute and *e.g.* vision and auditory feedback help compensate for the proprioceptive loss. Indeed, the case study of Ian Waterman (IW) brought the field of computational modeling of neuromotor control to a new level, when it became apparent that it was possible to sensory-substitute the absent motor reafference with visual and / or auditory inputs to update the motor commands and perform activities of daily living.

We had the opportunity to test IW within the context of co-adaptive learning using a Brain Computer Interface and here ask what the brain activity patterns would be in relation to participants who had intact proprioception. In this BCI context, the task was to learn to mentally control the external computer cursor and correctly move it to the left or to the right, upon instruction. Random order of instructions allowed the brain to accumulate activity in response to errors and successes,

such that gradually, working with the computer adaptive algorithm, it was possible to entirely phase out the algorithm and let the brain activity alone be the control signal. In the case of IW, we were curious to quantify this process, given that in controls we already knew that they were not only capable of learning the cursor control task under visual guidance, but most important was that the success strategy automatically transferred to the auditory domain [12]. In other words, all participants in our prior work were exclusively trained through visual input, yet when probed with eyes closed and instructed through audio, they all had 100% accuracy of cursor control: if instructed right/left, the cursor moved to the right/left even though auditory training never took place.

How would the visually guided version of this task be performed by IW? In the absence of bodily kinesthetic reafference and his well-documented heavy reliance on visual feedback, would his brain patterns differ from neurotypical participants?

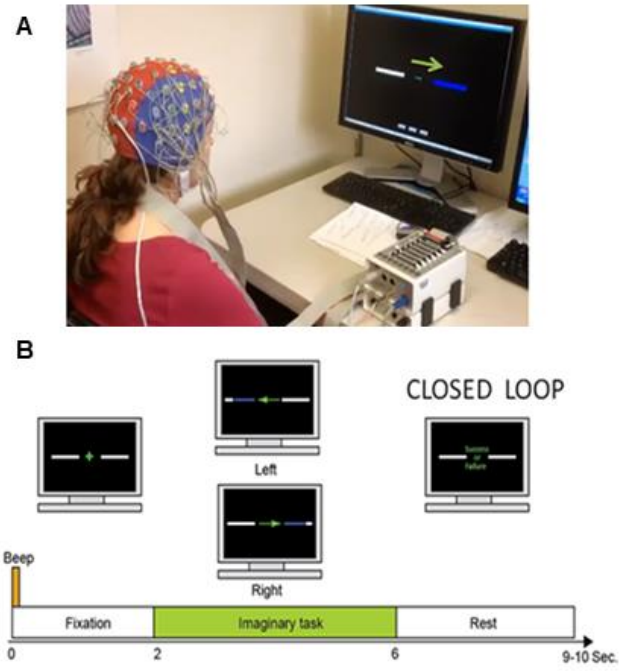

Figure 1: Experimental set up in which the subject sat comfortably in front of a computer screen. EEG data was recorded from 64 channels in response to the imagination of a visually instructed direction (arrow). The task was to control the arrow by moving it to the visually instructed direction (left or right arrow on the screen). Bottom row is the timeline of the task (in seconds.) Each trial is 10 seconds long (7 blocks with 30 trials each).

In the closed loop training phase, subjects were provided with visual feedback displayed on the screen at the end of every trial with a text string ("SUCCESS" or "FAILURE") based on whether they correctly moved the cursor to the intended (instructed) direction. This BCI updates the classifier within every trial. There are 7 blocks of 30 trials each, performed in the closed loop phase of training, which lasts 35 minutes. Further details on the classifier are described in [12].

This kind of closed loop training activity, whereby EEG signals adapt to the feedback and trains the classifier with every trial reveals the learning progression through the EEG activity. In this paper, we focus our analyses on the data from the closed-loop version of training, having 7 blocks of 30 trials each. Here, initially the algorithm (sparse

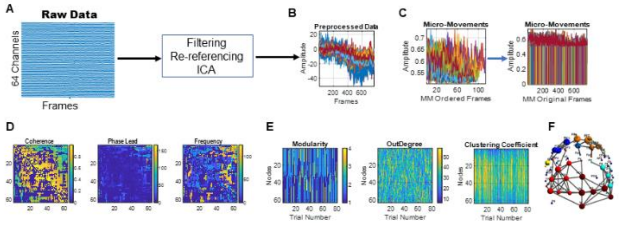

Figure 2: Analytical pipeline. (A) Raw EEG data (64 channel) collected for 1 sample trial. Pre-processing done in EEGLAB toolbox using the steps shown to remove artifacts and noise components in 63 channels (one for re-referencing.) (B) Peak extraction and amplitude scaling (C) to obtain "micro-movement" spike trains (MMS). (D) Pairwise maximum cross-coherence matrix with corresponding lead-lag and frequency matrices (constructed with convention that node from row *i* leads node from column *j*) provides adjacency matrix to represent weighted directed graphs and perform network connectivity analyses in (E). (F) Sample brain connectivity visual using the connectivity metrics we obtained in E.

probit classifier [10-11]) dominates, then gradually the brain dominates, while the classifier adapts to the intended brain activity that maximizes the accurate (volitional) control of the cursor's direction. We coin the first 80 trials *Machine Phase*, trials 65-145 *Hybrid Phase* and trials 130-210 *Brain Phase*. In the Machine Phase the algorithm dominates, in the Hybrid Phase we have the mixed actions of the brain and the classifier and in the Brain Phase, where the brain dominates over the algorithm, we interrogate the signals from IW *vs*. representative controls. In this work, we set 15 overlapping trials from phase to phase, to relax our prior assumption of independent identically distributed (iid) random process for the trial-by-trial time series analyses. This also makes smoother transition between different learning phases.

C. Methods

We focus here on the closed loop training phase (7 blocks of 30 trials each) free from eye movements, muscle movements, and power-line frequency artifacts. Pre-processing of this EEG data to remove unwanted signals generated from these artifacts was done for a prior publication. To that end, we used a standard EEG data pre-processing software called EEGLAB [13]. Briefly, the 64 channels data is filtered in a range of 0.1 to 50 Hz to avoid power-line frequencies captured by electrodes at 60 Hz using the function *FIR* for filtering. To keep the values of all channels with respect to the same ground truth and comparable to each other, we need to do re-referencing of electrodes. EEGLAB was used again to do the re-referencing and electrode Cz was chosen as the reference electrode. Electrode Cz's activity was subtracted from every electrode and was eliminated thereafter, leaving 63 electrodes.

Finally, we performed independent component analysis (ICA [14]) to separate all the additive components of the signals we harnessed from the leads (channels). It is assumed that the components are statistically independent of each other. The purpose of doing ICA decomposition is to get rid of the artifacts remaining in the signals after filtering for instance, eye blinks, ear muscle movement etc. To perform ICA decomposition, we used EEGLAB built-in function called *RunICA*. There are data from 63 electrodes for 210 trials (7x30), where each trial has 768 frames. Given, the sampling frequency of 256 Hz, each trial lasts for 3 seconds and each block is 90 seconds (1.5 minutes) long. Overall, we have the brain activity for 10.5 minutes (1.5x7) from the pre-processed data. These pre-processing steps along with

complete data analysis pipeline further are summarized in **Figure 2**.

The EEG data obtained after pre-processing consists of time series of peaks and valleys with varying amplitude and timing. We fit the frequency histogram from all peaks across all trials of a person to the best continuous family of distributions in a maximum likelihood estimation MLE sense (with 95% confidence.) Then the empirically estimated mean is used to mean shift the original peak amplitude data and centered at the empirically estimated mean. In this case, the continue Gamma family fit well in an MLE sense. These fluctuations in signal amplitude are scaled to the real valued interval [0,1] using the equation below [15,16]:

$$NormPeak = \frac{Peak}{Peak+Avrg_{min-to-min}} \qquad (1)$$

They give rise to a new waveform called the micro-movements spikes (MMS.) These MMS are used as the input to a random process under the general rubric of Poisson random process, with relaxed iid assumption. We sample continuously in identically sized blocks with overlapping sliding window and estimate the Gamma parameters (shape and scale), thus tracking their shift over time [15]. The MMS capture the absolute deviations from the empirically estimated mean, thus reducing the number of frames. To maintain the original number of frames, we zero-pad those frames which are not picked up and this enables *e.g.* pairwise cross-coherence analyses using nodes' activities using equal number of the original frames for each node.

The MMS datatype offers an individualized approach to work with these EEG signals as they account for all possible allometric effects due to different anatomies of participants heads [16].

We then use the MMS trains to build adjacency matrices and borrow concepts from weighted connected graphs[17] to build interconnected, dynamically evolving networks and perform connectivity analyses. To that end, we use the brain connectivity toolbox in Matlab [17] and derive connectivity metrics.

The adjacency matrices in **Figure 2D** were obtained from pairwise cross-coherence analyses on the leads (nodes) by choosing the maximum cross-coherence value and its corresponding frequency and phase lead values. This procedure yielded 3 63 x 63 matrices for each trial. Each entry in the matrix represents the maximum cross-coherence value between the pair of lead nodes (given by row *i* and column *j*) for that trial. The phase lead-lag matrix gives the phase value (in degrees) when maximum cross-coherence occurs between the corresponding pair of nodes. Similarly, the frequency matrix gives the frequency value when the maximum coherence occurs between the corresponding pair of nodes. We adopt the convention that positive leads indicate row node *i* leads the column node *j*. These adjacency matrices are then used to build the weighted directed graphs and we derive connectivity metrics such as *Betweenness Centrality*, *Clustering Coefficient*, *InDegree*, *OutDegree*, *TotalDegree*, *InStrength*, *OutStrength*, *TotalStrength*, *Modularity*, etc. These connectivity metrics and others involving phase locking value (PLV) [18] are used to generate connectivity visuals with the help of Brain Net Viewer (BNV) toolbox [19] as in **Figure 2F** using as input the connectivity metrics that we obtained. The node size is represented by *OutDegree*, the node color by module participation, edge thickness and direction by value of phase under our convention $i \rightarrow j$, and edge color may be used to *e.g.* represents coherence value.

These brain connectivity visuals offer a glance at the differences in connectivity with and without proprioception. In addition, we further investigate the amount of dynamic change in brain activity over the course of learning. To that end, we use a distance metric measuring the amount of effort that it takes to convert one frequency histogram to another [20,21], whereby the MMS peaks of a trial produce the histogram for that trial. Specifically, we use the earth mover's distance (EMD) metric between histograms produced by two consecutive trials, thus building a series of numbers reflecting the pairwise similarity of spiking activity from moment to moment. In this context the EMD reflects stochastic change in the brain activity (via the change in distributions of MMS) in the amplitude domain. We group the 63 nodes according to 13 conventional brain regions: LPF- Left PreFrontal, LF- Left Frontal, LC- Left Central, LT- Left Temporal, LO- Left Occipital, LP- Left Parietal, : RPF- Right PreFrontal, RF- Right Frontal, RC- Right Central, RT- Right Temporal, RO- Right Occipital, RP- Right Parietal, CC- Corpus Callosum).

III. Results and Discussion

Figure 3 shows the connectivity visuals for Ian Waterman (IW) derived from the Brain phase and shown in relation to that phase for two representative participants, JN a biologist and IY a Mathematician. IW has a densely connected network compared to JN and IY in the initial learning and this density evolved throughout the co-adaptive learning. There are differences in the rate of change in learning as well (**Figure 4**), whereby IW shows higher changes according to the EMD for each learning phase. **Figure 4** shows this evolution for the participants in **Figure 3**.

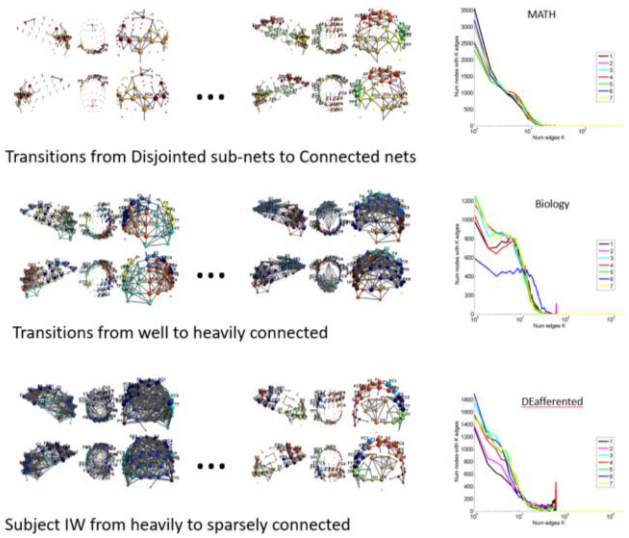

Figure 3. Evolution of brain's network activity in two representative participants, a mathematician and a psychologist in relation to IW. Left hand panels show the initial brain activity in the first block (machine) *vs.* the activity in the last block (brain) using the connectivity output for PLV-based adjacency matrix to build the networks. Right hand graphs show the evolution in network topology through the degree distributions reflecting the number of edges K in the network *vs.* the number of nodes with K edges evolving for the 7 blocks.

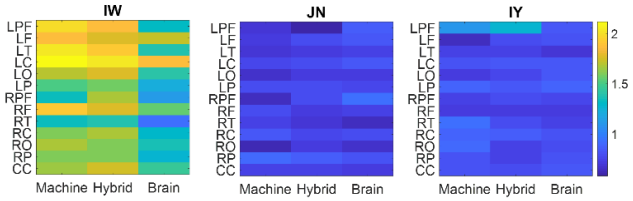

Figure 4: Amount of change in brain activity for IW in relation to the representative participants of **Figure 3**. EMD metric was used to build these matrices using the orderly trial by trial "*effort*" to change one MMS histogram into another. Each column represents a learning phase. IW shows more changes in trial-by-trial probability distribution of MMS, as quantified by the EMD metric (unitless quantity from normalized MMS coded in the color bar.)

IV. CONCLUSION

This paper tracked the neuro-dynamics of co-adaptive learning in the context of BCI, as neurotypical participants mastered the control of an external cursor direction on a computer screen. The task probed two randomly instructed directions (left *vs.* right, randomly presented with equal probability) guided by accuracy, visually displayed. Based on this visual outcome (success or failure) the participant's brain in tandem with the algorithm gradually transitioned from machine to hybrid to purely brain signal-based control. The comparison of this process to IW revealed large differences in connectivity patterns and in the amount of change that ensued from trial to trial. Specifically, IW showed higher connectivity patterns all throughout the learning process and higher moment-by-moment changes in MMS variability (stochastic change.)

We interpret these results as higher cognitive load and higher capacity to process sensory signals when sensory substitution (by visual information in this case) is used to compensate for the loss of re-afferent feedback. Although this task does not require overt movements, covert minute motions across the body exist to sustain the body upright, to maintain the body posture steady throughout the experiment. In the absence of proprioception, IW must do that deliberately through vision, in addition to utilizing the visual input to track accuracy and master the cursor control at will. Indeed, he mastered the control as did the other neurotypical participants with intact proprioception. Yet the excess activity and changes in patterns of variations, lead us to suggest that he mastered this feat under much higher cognitive load than the average person would. Since his capacity for cognitive control is not diminished by the absence of kinesthetic afference and the loss of proprioception, we posit that his brain must be tapping into resources that we do not often use -as instantiated by the brain activity patterns.

There is a myth that we only use 10 percent of our brain, as not all neurons fire during the execution of complex motions and long mathematical calculations. Recruiting the full brain for a seemingly simple cursor control task such as this one – a task that requires no overt bodily motion or no complicated cognitive calculations, would then be for IW analogous to recruiting all muscles while sprinting, or while performing highly complex mathematical computations. Perhaps IW's brain does that while his nervous system sensory substitutes. In so doing, his brain may have mastered the use of the other 90 percent. Further research will help us better unravel this mystery about "*The Man Who Lost His Proprioception*" [6] and contributed to our enlightenment on how the brain can attain agency.

ACKNOWLEDGMENTS

This research was funded in part by a grant from Rutgers TechAdvance Funds and by the Nancy Lurie Marks Family Foundation Career Development Award to EBT. We thank IW for his contribution to science.

V. REFERENCES

1. Kawato, M., Wolpert, D.M. *Internal models for motor control.* Novartis Found. Symp, 1998. **218**: p. 291-304; discussion 304-7.
2. Wolpert, D.M., Kawato, M., *Multiple paired forward and inverse models for motor control.* Neural Networks, 1998. **11**(7-8): p. 1317-29.
3. Wolpert, D.M., Miall, R.C. and Kawato, M., *Internal models in the cerebellum.* Trends Cogn Sci, 1998. **2**(9): p. 338-47.
4. Von Holst, E., Mittelstaedt, H. (1950) *The principle of reafference: Interactions between the central nervous system and the peripheral organs. In:* Perceptual Processing: Stimulus equivalence and pattern recognition (Dodwell PC, ed), pp 41-72. New York: Appleton-Century-Crofts.
5. *(Author-Elsevier)*
6. Cole, J., *Pride and a daily marathon*. 1st MIT Press ed. 1995, Cambridge, Mass.: MIT Press., 194 p.
   Cole, J. (1998) *Rehabilitation after sensory neuronopathy syndrome*. J R Soc Med 91:30-32.
7. Cole, J.D., Paillard, J. (1995) *Living without touch and peripheral information about body position and movement: studies with deafferented subjects.* In: The body and self (Bermudez JL, Marcel AJ, eds), pp 245-266. Cambridge: MIT Press.
8. Cole, J.D., Sedgwick, E.M. (1992) *The perceptions of force and of movement in a man without large myelinated sensory afferents below the neck*. J Physiol **449**:503-515.
9. Cole, J.D., Merton, W.L., Barrett G, Katifi HA, Treede RD (1995) *Evoked potentials in subject with a large-fibre sensory neuronopathy below the neck*. Can J Physiol Pharmacol **73**:234-245.
10. Balakrishnan, S., Madigan, D. (2008) *Algorithms for sparse linear classifiers in the massive data setting*. Journal of Machine Learning Research **9**:313-337.
11. Ding, Y., Harrison, R.F. (2011) *A sparse multinomial probit model for classification*. Pattern Analysis and Applications **146**:47-55.
12. *(Author -JNeurophys)*
13. Makeig, S., Debener, S., Onton, J., Delorme, A. (2004) *Mining event-related brain dynamics*. Trends in Cognitive Science **8**:204-210
14. Bell, T., Sejnowski, T., (1997) *The "independent components" of natural scenes are edge filters*. Volume 37, Issue 23, December 1997, Pages 3327-3338
15. *Author (Frontiers)*
16. Lleonart, J.; Salat, J., Torres, G.J. *Removing allometric effects of body size in morphological analysis*. J. Theor. Biol. 2000, **205**, 85–93.
17. Sporns, O., Networks of the Brain (2010). MIT Press
18. Aydorea, S., Pantazis, D., Leahy, R.M. (2013), *A note on the phase locking value and its properties.* NeuroImage **74**, Pages 231-244
19. Xia. M., Wang, J., He, Y. (2013) *BrainNet Viewer: A Network Visualization Tool for Human Brain Connectomics*. PLoS ONE **8**(7): e68910. https://doi.org/10.1371/journal.pone.0068910
20. Monge, G. *Memoire sur la theorie des deblais et des remblais*. In Histoire de l' Academie Royale des Science; avec les Memoired de Mathematique et de Physique; De L'imprimerie Royale: Paris, France, 1781.
21. Rubner, Y., Tomasi, C., Guibas, L.J. *Metric for Distributions with Applications to Image Databases*. In Proceedings of the ICCV 1998, Bombay, India, 4–7 January 1998.